# Volumetric Analysis and Characterization of D_7 Reservoir using Well log and Seismic Data

**Omoregbe, O.A*, Oloyede, D.A**, and Momoh, H.N****

* Resemco Limited
** Geology Department, University of Benin

DOI: 10.29322/IJSRP.10.07.2020.p10308
http://dx.doi.org/10.29322/IJSRP.10.07.2020.p10308

***Abstract***- Suites of wire-line logs from seven (7) wells were integrated with 3D seismic data in order to characterize reservoir D_7 and estimate its hydrocarbon volumes. Detailed seismic interpretation was carried out to determine geologic structures. Seismic-to-well tie was done using previously generated synthetic seismogram, and this was used to pick the reservoir horizons; time and depth structural maps were subsequently generated. Geostatistical models were built using the Sequential Indicator Simulation and Sequential Gaussian Simulation which resulted in improved distribution of reservoir properties within the geologic cells. Statistical analysis of Porosity, Water saturation and Net-to-gross models for the reservoir revealed porosity values ranging from 18% to 27%, average water saturation of 45% and mean Net-to-gross value of 70%. Furthermore, the structural model showed a fault assisted closure. Finally, volumetric estimation revealed a STOIIP of 84Mstb. The results of this study has shown good hydrocarbon potential of reservoir D_7.

***Index Terms***- Geostatistical, Hydrocarbon, Reservoir, Seismic.

## I. INTRODUCTION

Reservoir modeling is an important tool which aids in planning and development of depletion strategies for hydrocarbon reservoirs. However, it is often associated with uncertainties that may lead to inadequate description of the reservoir and prediction of field performance. Integrating seismic and well data sets will help in providing subsurface images that will aid geological interpretation and ultimately reduce uncertainties (Oluwadare *et.al*, 2017). Moreover, successful integration of relevant data depends on its quality. Optimizing reservoir management and field development requires a model capable of realistically predicting the dynamic behaviour in terms of fluid recovery and production rate for different operating conditions. Reservoir modeling and characterization focuses on integrating all available geologic data and subsequent interpretation that would aid in unraveling the nature of subsurface environments. Geostatic models are very useful in estimating reservoir properties and are also required as input to reservoir simulation programs which predict the movement of fluids within the reservoir under various hydrocarbon scenarios. It is essential to model the reservoir as accurately as possible in order to calculate the reserves and to determine the most effective way of recovering the hydrocarbon as economically as possible (Lucia and Fogg, 1990; Worthington, 1991; Haldersen and Dasleth, 1993).

This study focuses on integrating well log and seismic data to effectively characterize the D_7 reservoir and estimate its hydrocarbon volumes.

### Geology of Study Area

The study area falls within the Niger Delta Basin. The Niger Delta Basin is a prograding depositional complex located in Southern Nigeria. It is bounded in the West by the Benin flank; the subsurface continuation of the West Africa shield, in the East by Calabar flank; the subsurface continuation of the Oban massif, to the North by Abakaliki and the post-Abakaliki (Anambra basin); and to the South by the Atlantic Ocean (Murat, 1972). Due to subsidence and deposition, a succession of transgressive and regressive sequence advanced south-west of the Niger Delta Basin (Oomkens, 1974) which resulted in the deposition of

between 9,000m to 12,000m thick transgressive/regressive sequences similar to the Gulf Coast Tertiary section in the United States of America (Curtis, 1970). Detailed information about the origin, geomorphology, tectonic setting, structural pattern, stratigraphy and depositional environment of the Niger Delta Basin has been provided by various authors (Reijers, 2011; Lehner and De-Ruiter, 1977; Kulke, 1995; Doust and Omatsola, 1990; Stacher, 1995; Michelle *et al.*, 1999; Damuth, 1994; Mascle *et al.*, 1973; Short and Stauble, 1967).

## II. METHODOLOGY

Seismic (3D cube) and well (headers, deviation, logs, and checkshot) data sets from seven (7) wells was used for this research study. They were interpreted and analyzed using the Petrel software. A detailed research methodology workflow is shown in Fig.1.

**Data Quality check and Importation**

The data sets were quality checked to ensure they were in the right format and then imported into the Petrel software platform (Table 1).

**Well Log Interpretation and Correlation**

The lithology was delineated using the gamma ray log which ranges from 0 API to 150 API. The shale formations have high radioactive contents, thus deflecting to the right of the baseline. While the sand formations deflect to the left of the baseline. The reservoir was also correlated across seven (7) wells.

**Seismic Interpretation**

Prominent geologic structures such as faults were identified across the seismic section. Geological fault interpretation was done on both inline and cross lines. The check shot data was used to generate a synthetic seismogram for well-to-seismic-tie (Fig. 3). The synthetic seismogram further aided in picking the top horizon of D_7 reservoir on both inline and cross lines. The mapped horizon was then used to generate a structural time map.

Two-Way Time (TWT) was plotted against True Vertical Depth (TVD) using a polynomial function of second order (Fig. 2). The equation generated was subsequently used to build a velocity model for converting the time structural map to depth structural map.

**Petrophysical Evaluation**

**Volume of Shale**: The volume of shale within the reservoir was determined from the gamma ray log by first calculating the gamma ray index using the equation below:

$$IGR = \frac{GR_{log} - GR_{min}}{GR_{max} - GR_{min}} \quad \text{Equation 1}$$

Where: IGR = gamma ray index, $GR_{LOG}$ = gamma ray reading of the formation, $GR_{MIN}$ = minimum gamma ray (clean sand), $GR_{MAX}$= maximum gamma ray (shale). The gamma ray index was then used to calculate the volume of shale using the Larinov tertiary rock equation

$$V_{shale} = 0.083 * (pow(2.(3.7 * IGR)) - 1) \quad \text{Equation 2}$$

**Porosity**: The total porosity gives the ratio of pore volume to the total volume of the reservoir. It was evaluated using Wyllie's equation.

$$\emptyset = (\rho_{ma} - \rho_b)/(\rho_{ma} - \rho_f) \quad \text{Equation 3}$$

Where $\rho_{ma}$ is the matrix density, $\rho_b$ is formation bulk density and $\rho_f$ is fluid density.

**Effective Porosity**: This was obtained using the equation below;

$$\emptyset_{eff} = (\emptyset \times (1 - V_{sh}) \quad \text{Equation 4}$$

Where $\emptyset_{eff}$ is effective porosity, $\emptyset$ is total porosity and $V_{sh}$ is volume of shale.

**Water Saturation**: This was estimated using the Archie's equation;

$$S_w = \sqrt{(R_w/(ILD \times \phi^{1.74})} \quad \text{Equation 5}$$

Where, $S_W$ = water saturation, $R_W$ = water resistivity and ILD = true resistivity.

**Permeability**: This refers to the movement of fluid within the interconnected pore spaces and was obtained using the equation;

$$K = [250\left(\frac{\emptyset^3}{Sw_{irr}}\right)]^2 \quad \text{Equation 6}$$

Where, K = permeability, $\emptyset$ = porosity and $Sw_{irr}$ = irreducible water saturation.

**Geostatic Reservoir Modeling**

Reservoir modeling workflow proceeds in stages which consist of structural modeling, facies modeling and petrophysical modeling.

**Table 1: Data file type and their formats**

| No. | DATA | DATA CATEGORY | DATA FORMAT (FILE TYPE) |
|---|---|---|---|
| 1 | Well | Well headers | Well heads (**) |
| | | Well paths/deviations | Well path/deviation (ASCII) (**) |
| | | Well logs | Well log (ASCII) (**) |
| | | Checkshot | Checkshot (ASCII) (**) |
| 2 | Well tops | | Well tops (ASCII) (**) |
| 3 | 3D Seismic | Horizon | Seismic data in (SEGY) |

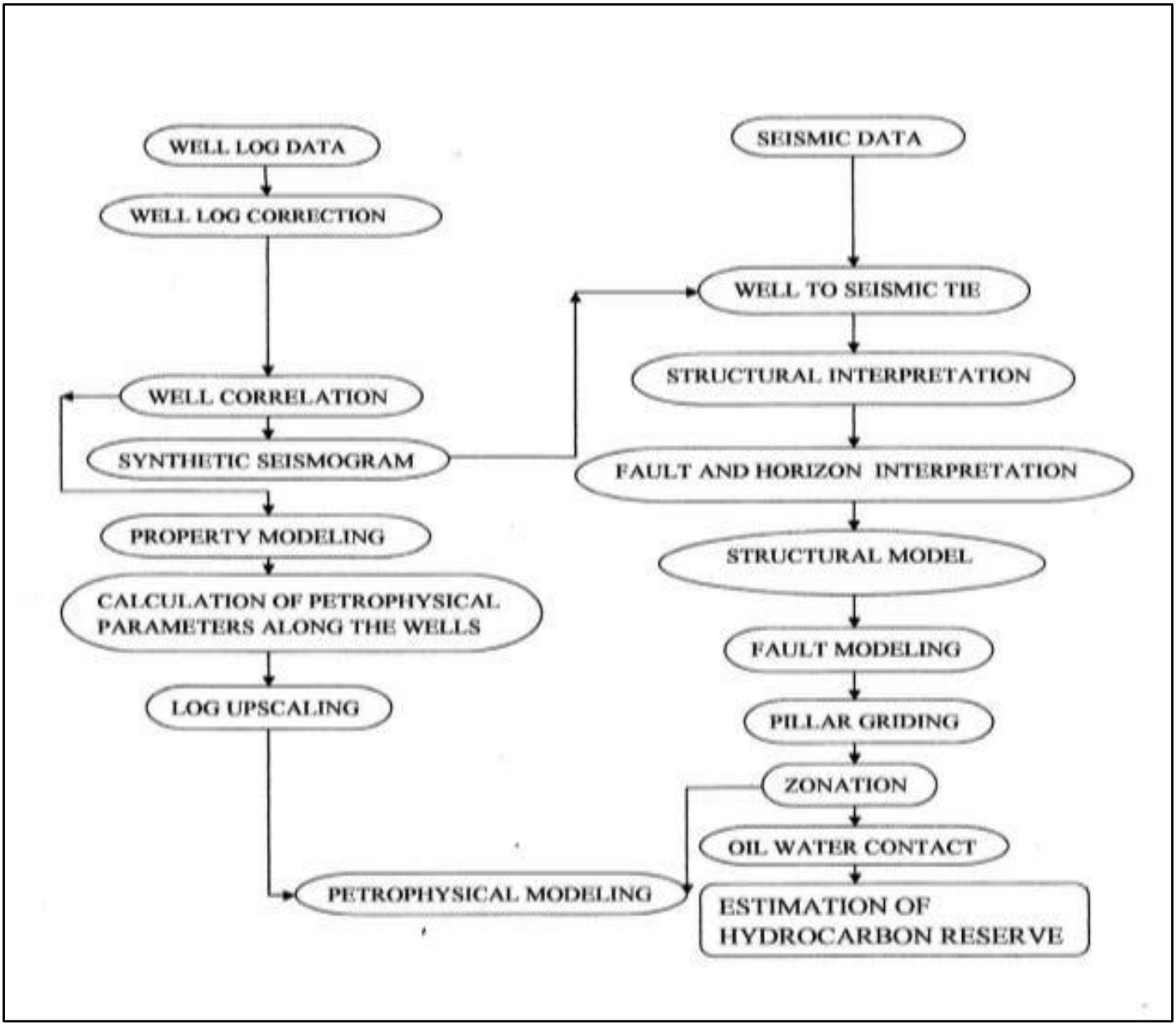


**Fig. 1:** Research Methodology Workflow

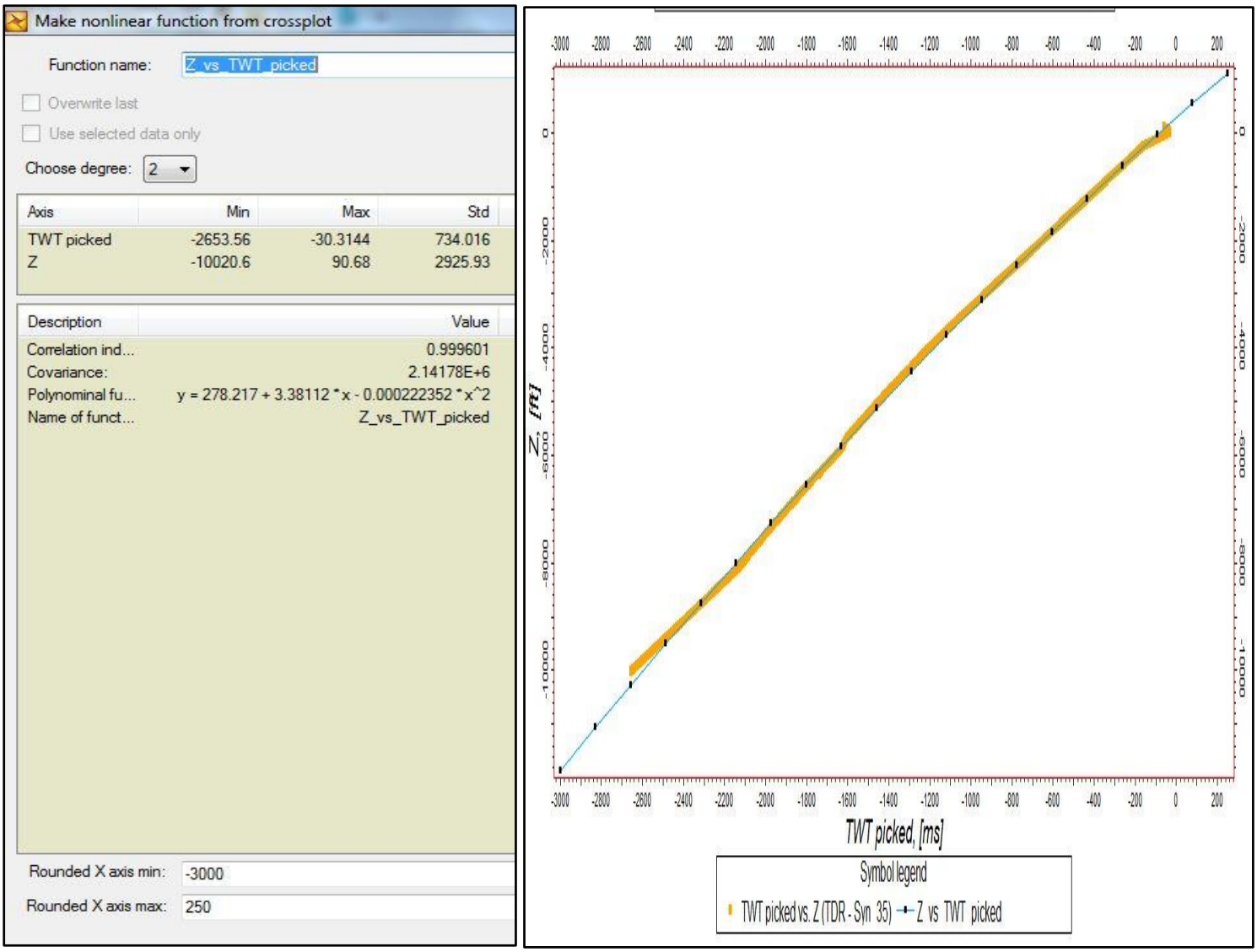


**Fig. 2:** Plot showing relationship between TWT and Z using the polynomial method

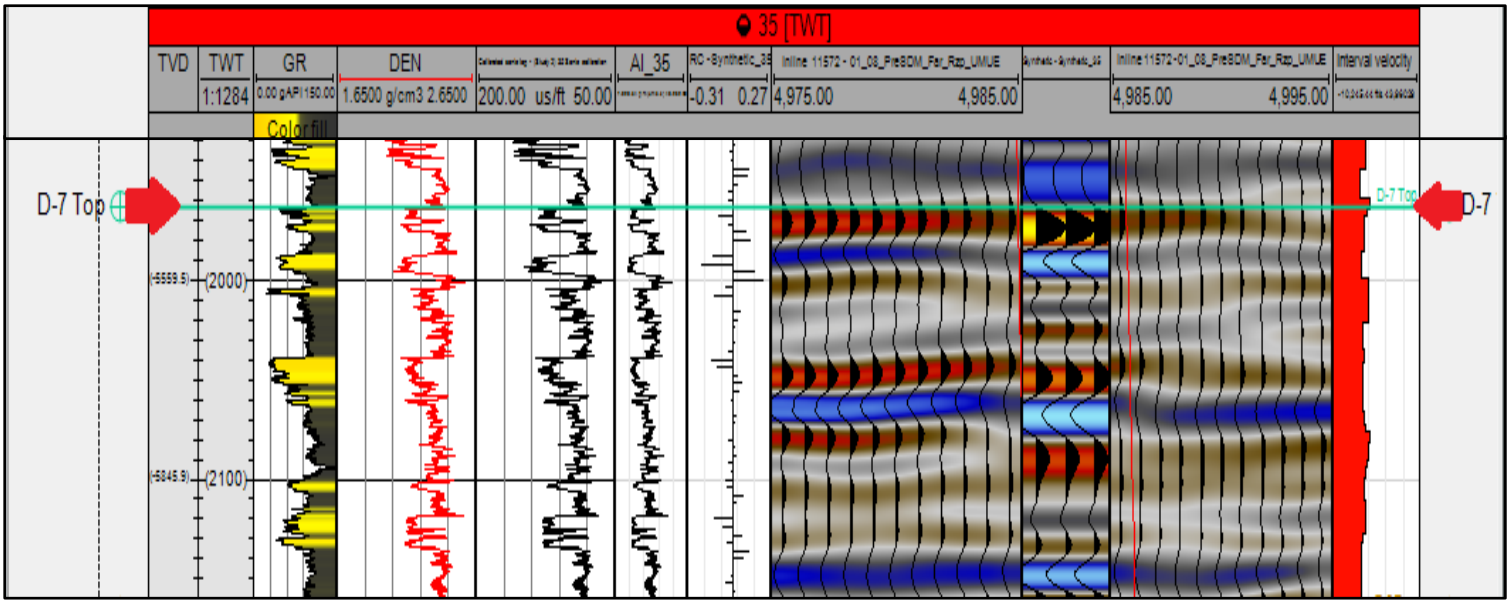


**Fig. 3:** Well-to-seismic-tie of reservoir D_7

**Structural Modeling**

This is the first step in building a geostatic model. Structural modeling comprises of fault modeling, pillar gridding, and layering.

- ***Fault Modeling***: This involves the definition of faults in the geological model that form the basis for generation of the 3D grid.
- ***Pillar Gridding***: Gridding involves creation of gridded surfaces from seismic interpretation, structural maps and faults.
- ***Layering***: This involves building stratigraphic horizons, zones, and layers into the 3D grid. For this study, horizons were defined using seismic surfaces as input data. Zonation is the process of creating the different zones from the surfaces.

**Up scaling of Well Logs**

This is the process of grid coarsening enabled by calculation of effective flow properties using analytical (arithmetic, geometric, harmonic averages) and numerical simulation. The properties included in the scale-up process for this study were porosity, water saturation, net-to-gross, and facies type. These properties were scaled up using arithmetic averaging. Sequential indicator simulation and sequential Gaussian simulation were employed to estimate values for cells between wells.

**Property Modeling**

This is the process of assigning petrophysical properties to grid cells. The layer geometry given to the grid during layering follows the stratigraphy of the model area. These processes are therefore dependent on the geometry of the existing grid. When interpolating between data points, Petrel software propagates property values along the grid layers. Property modeling is divided into two separate processes; Facies and Petrophysical Modeling**.**

- **Facies Modeling**: This is a means of distributing discrete facies throughout the model grid. In this study, facie modeling was done using the sequential indicator simulation algorithm. Two major facies type (shale and sand) were defined on the basis of reservoir property relationships and this was used to populate the geocellular model of the D_7 reservoir.
- **Petrophysical Modelling**: The purpose of petrophysical modeling is to distribute properties between the wells so that it realistically preserves the reservoir heterogeneity and matches the well data. This comprises of porosity, net-to-gross, volume of shale and water saturation models.

**Reservoir Volumetric Estimation**

This was done using the equation below;

$$STOIIP = \frac{7758 \times Ah\emptyset(1-S_w)NTG}{B_o} \quad \ldots\ldots\ldots\ldots \quad Equation\ 7$$

Where;

7758 = Area constant in acres/ft.

A = Area of pay zone,

h = Pay thickness,

$S_w$ = water saturation,

N/G = Net-to-gross

Bo = Oil formation volume factor

Ø = porosity

## III. RESULTS AND DISCUSSIONS

**Reservoir Geology**

D_7 reservoir was correlated across the seven (7) wells (25, 3, 60, 65, 2, 58 and 35 respectively) along the dip direction (SE) (Fig. 4). This was done using both gamma ray and resistivity logs. Hydrocarbon bearing intervals and fluid type (oil, gas or water) were identified using resistivity, neutron and density logs. The correlation panel showed the sands thinning out with presence of shale intercalations towards the S-E direction. This is probably an indication of shoreface sands prograding into marine; a characteristic of deltaic environments (Fig. 5 and 6). Reservoir tops and bases were delineated using GR, neutron and density logs (Table 2).

**Structural Interpretation**

From the study it was revealed that the reservoir has a rollover anticline structure with dip closure to the East and West bounded by growth faults to the North and North-west located on the footwall of the major growth fault. The regional growth fault is an elongate East-west trending fault that assisted the reservoir in trapping hydrocarbon.

**Table 2**: Tops, Bases, Contacts and Petrophysical Information of Reservoir D_7

| Wells | Top (ft.) | Bottom (ft) | OWC (ft) | Thickness (ft) | Pay Thickness (ft) | NTG | Ø | $S_w$ |
|---|---|---|---|---|---|---|---|---|
| **Well 25** | 7579 | 7746 | | 167 | | 0.82 | 0.21 | 0.99 |
| **Well 03** | 7570 | 7700 | | 130 | | 0.47 | 0.15 | 0.79 |
| **Well 60** | 7628 | 7724 | | 96 | | 0.64 | 0.21 | 0.99 |
| **Well 65** | 7313 | 7365 | 7326 | 52 | 13 | 0.65 | 0.21 | 0.66 |
| **Well 02** | 7382 | 7460 | 7406 | 78 | 24 | 0.38 | 0.13 | 0.54 |
| **Well 58** | 7270 | 7331 | 7329 | 61 | 59 | 0.53 | 0.18 | 0.38 |
| **Well 35** | 7308 | 7373 | 7378 | 65 | 70 | 0.39 | 0.16 | 0.42 |

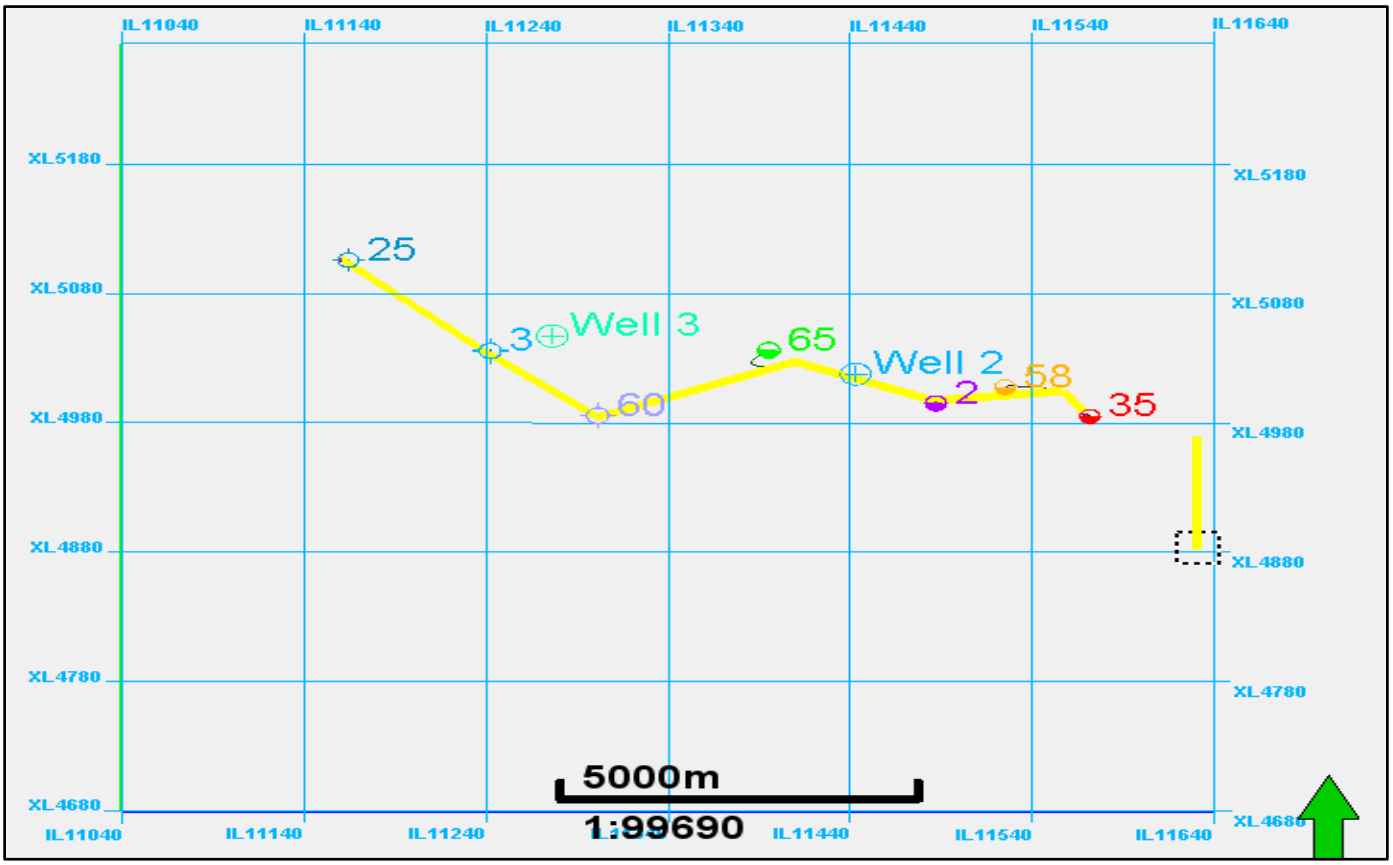


**Fig. 4:** Base map showing cross-section of the correlated wells

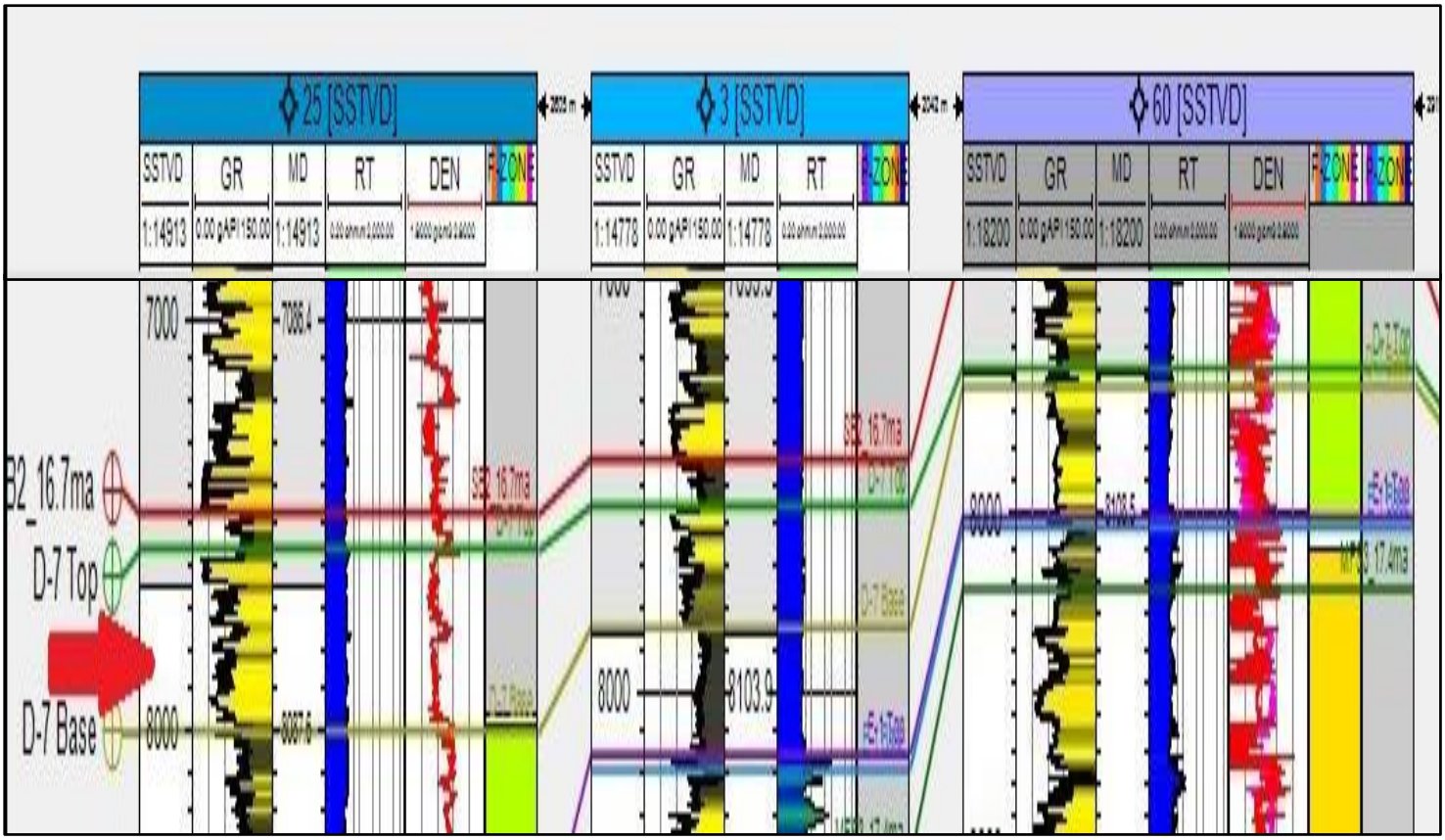


**Fig. 5:** Correlated well section (wells 25, 3 and 60) showing top and base of reservoir

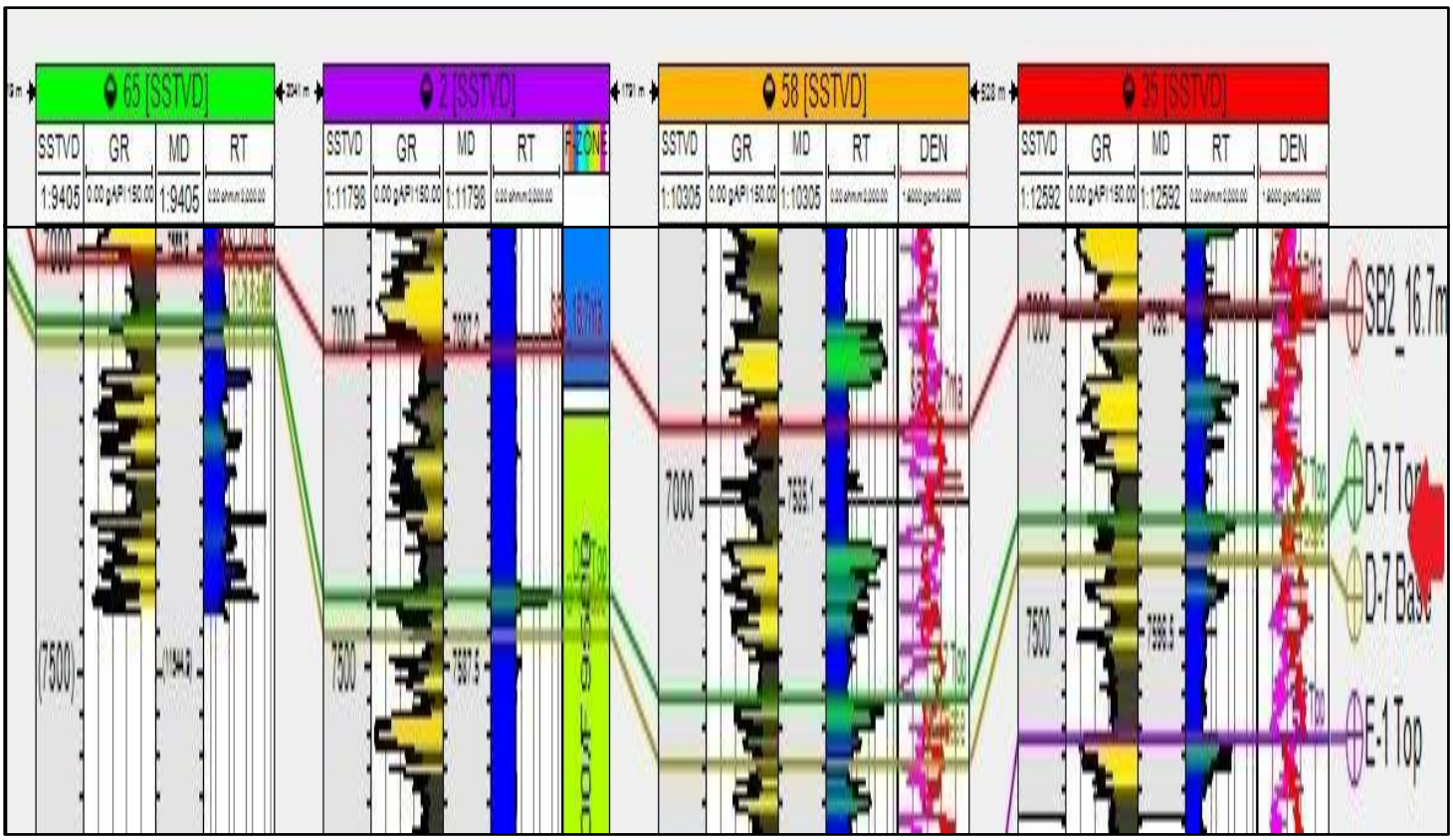


**Fig. 6:** Correlated well section (wells 65, 2, 58 and 35) showing top and base of reservoir

A major fault trending NW-SE was identified with several synthetic faults (Fig. 7). The closure within this reservoir was observed to be fault assisted and serves as a seal preventing further migration of the hydrocarbon (Fig. 8 and 9).

**Stratigraphic Interpretation and Depositional Environment**

The well logs and facies model showed a predominantly deltaic (paralic facies) comprising of shoreface/ barrier bar and channel sands depicted by a coarsening upward gamma ray log signature. This was further corroborated by lateral continuity of the sand package; typical of shoreface deposits. The facies model indicates abundance of shoreface sand deposits in the south-eastern part of the reservoir (Fig. 10). The gamma ray log also shows that the sand packages are thicker in the west and thins out eastward which is suggestive of a shelf to slope depositional environment. The shale distribution on the model suggests that a large scale flooding occurred during transgression.

**Reservoir Thicknes**

Reservoir D_7 was delineated in well 25 at a depth interval of (7579-7746ft), well 03 at (7570-7700), well 60 at (7628-7724ft), well 65 at (7313-7365ft), well 02 at (7382-7460ft), well 58 at (7270-7331ft), and well 35 at (7308-7373ft). This information was used to generate the thickness (isochore map). The isochore map shows that the reservoir is thicker in the West and thins out towards the East (Fig. 11).

**Petrophysical Interpretation**

This was done to generate the water saturation model, porosity model and the net-to-gross model.

**Water Saturation Model**

This shows water saturation distribution within the reservoir to range from 38% to 99%. Wells 25 and 60 showed the highest water saturation, while well 58 had the lowest water saturation of 38% (Fig. 12).

**Porosity Model of Reservoir**

Porosity distribution ranges from 13% to 27%. This indicates that reservoir D_7 has good porosity for accumulation of hydrocarbon (Fig. 13).

**The Net-to-Gross Model**

The net pay was deduced from the net to gross distribution. The net-to-gross model depicts highest net to gross ratio of 72%-80%, and lowest net to gross value of 25% - 45%. Due to the poor net-to-gross ratio of the reservoir in wells 25 and 60, production may not be economical enough. However, wells 35, 2, 58 may be good producing wells due to high net-to-gross ratios (Fig. 14). This only gives an idea about the producing capabilities of the wells penetrating the reservoirs. Final decisions should not be based on this alone.

**Fluid Contact and Volumetric Estimation**

The hydrocarbon contact was delineated from the well logs (gamma, resistivity and density-neutron). The density-neutron log revealed Oil-water contact (OWC), no Gas-oil contact was observed since the logs showed that the reservoir is an oil reservoir with no gas. Wells 65, 02, 58, and 35 had fluid contacts at 7326ft, 7406ft, 7329ft, and 7378ft respectively. However, fluid contacts in wells 25, 03, and 60 could not be effectively determined because their resistivity logs were not available and the density-neutron logs had poor signals. Hydrocarbon volume was calculated and stock tank oil initially in place (STOIIP) value of 84Mstb was obtained as shown in Table 3.

## IV CONCLUSION

The integration of all available data (geophysical, geological, petrophysical) has led to the building of a consistent geostatic model of the reservoir which can used in field development planning and may also serve as input into a 3D dynamic reservoir simulation model. The reservoir characterization has led to detailed description and understanding of the reservoir which is very important in developing an efficient reservoir management strategy. Well logs used for this study includes Gamma ray, Resistivity, Neutron and Density logs. The seismic interpretation showed a highly faulted closure for hydrocarbon entrapment and accumulation. Petrophysical analysis revealed good reservoir properties. Volumetric estimation showed good and economically viable hydrocarbon yield. The depositional environment suggests a deltaic environment due to the presence of prograding shore sands and channel sands intercalated with shales.

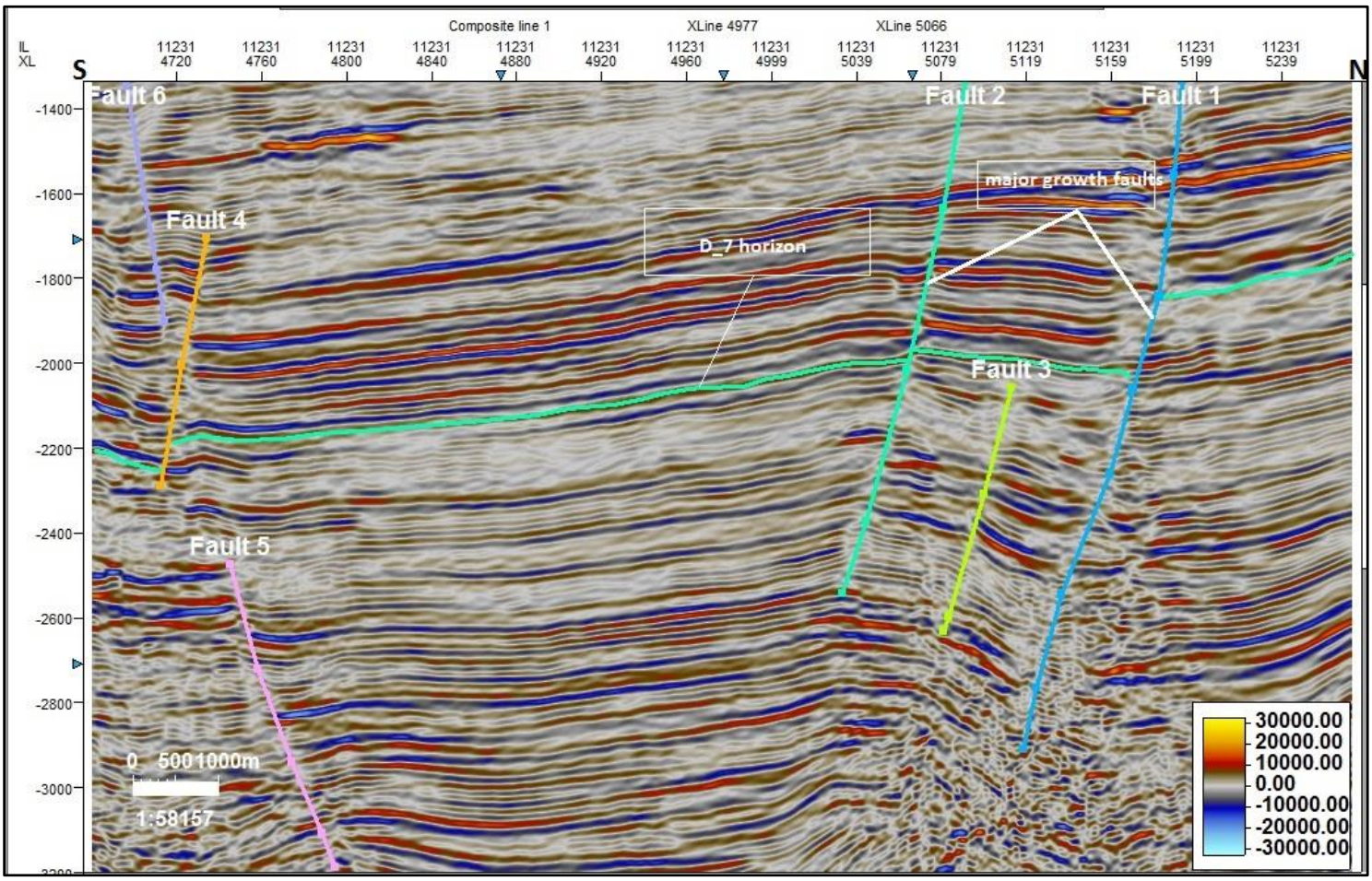


**Fig. 7a:** Seismic section showing the faults and reservoir horizon

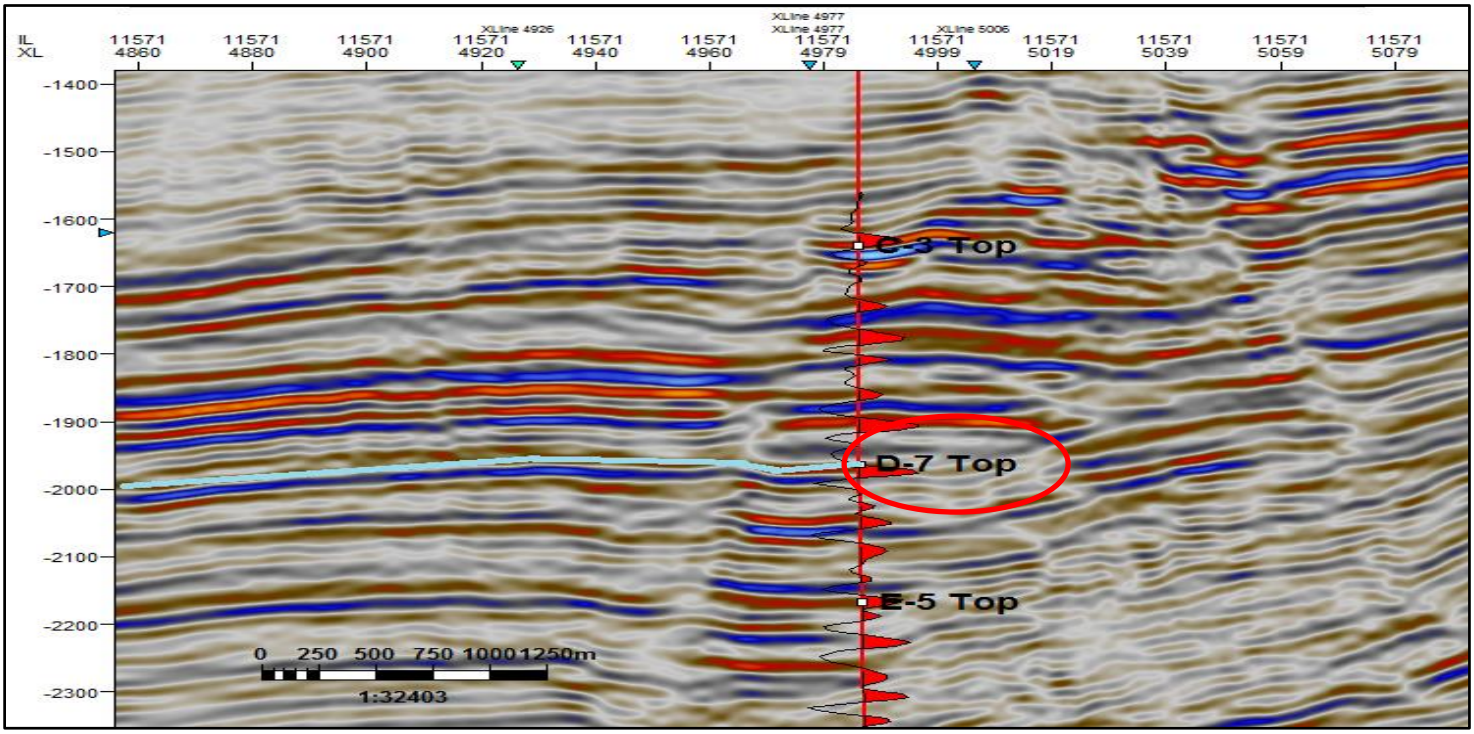


**Fig. 7b:** Seismic section showing reservoir D_7 horizon

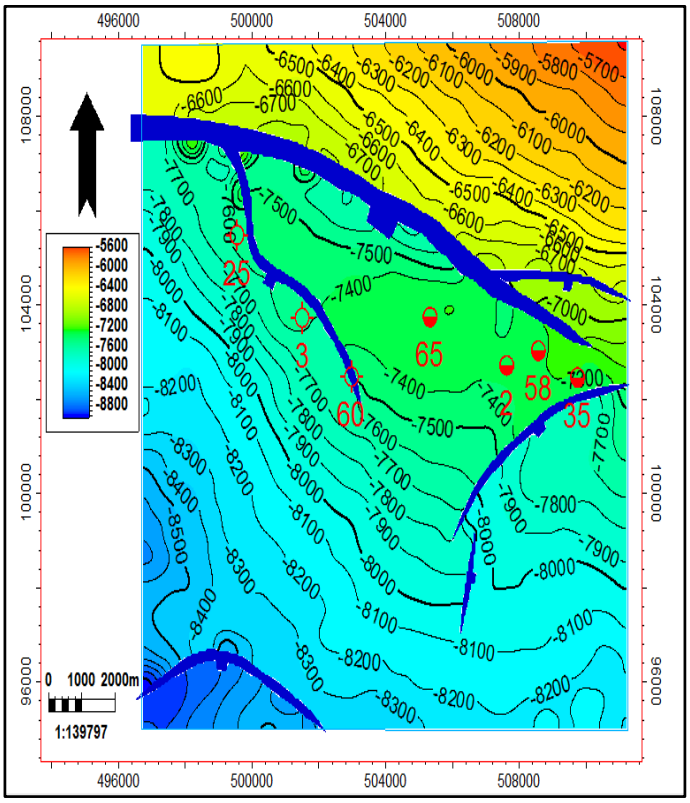


**Fig. 8:** Structural depth map for reservoir Top

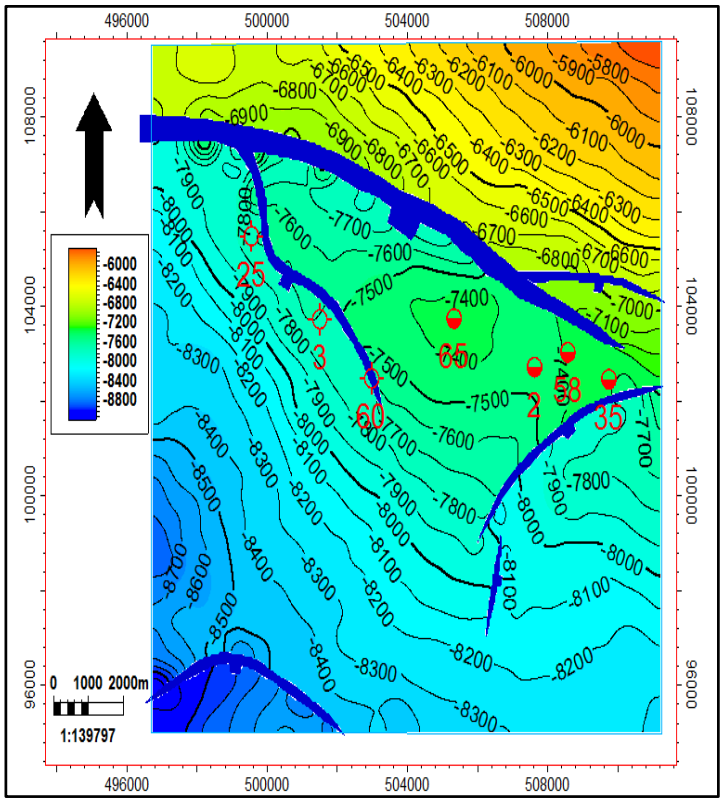


**Fig. 9:** Structural depth map for reservoir Base

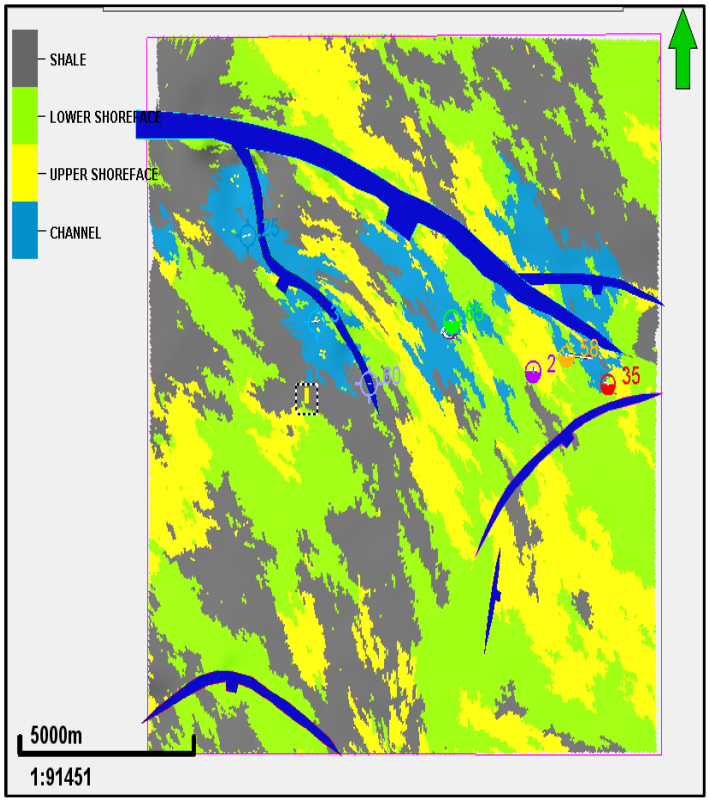


**Fig. 10:** Facies distribution map

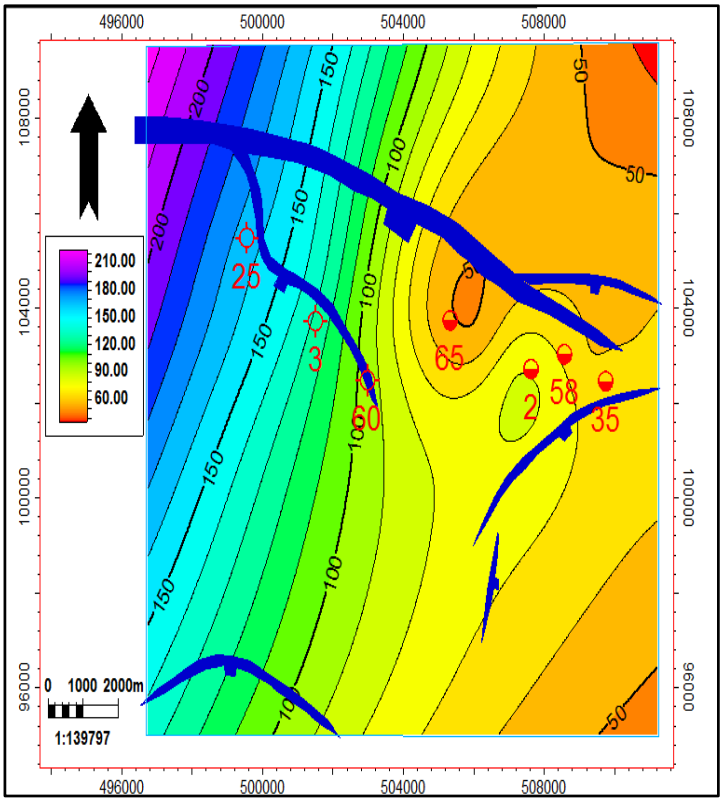


**Fig. 11:** Thickness map

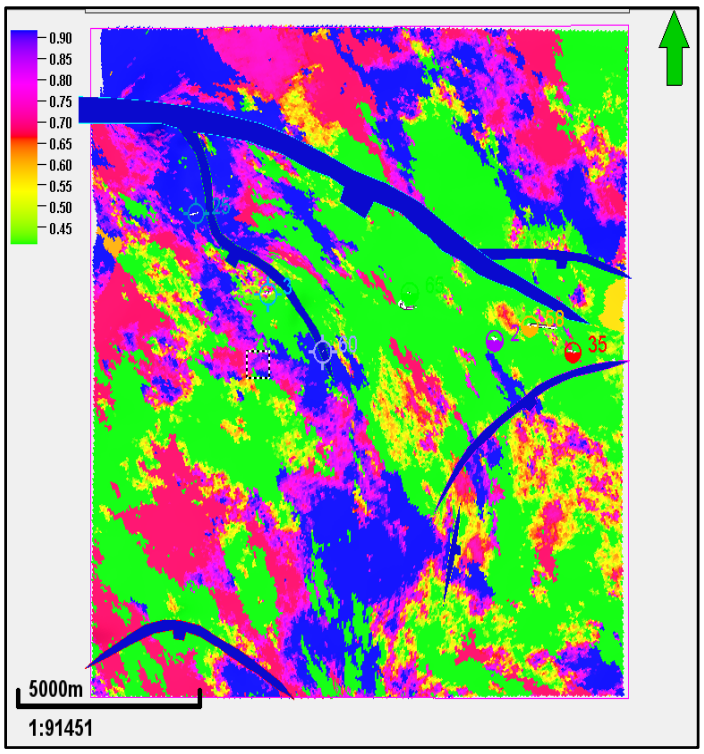


**Fig. 12:** Water saturation model

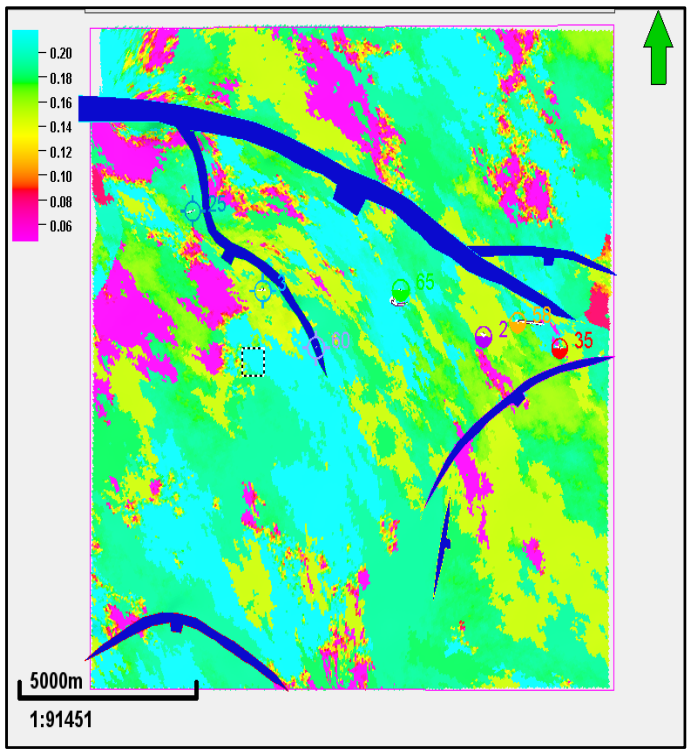


**Fig. 13:** Porosity model

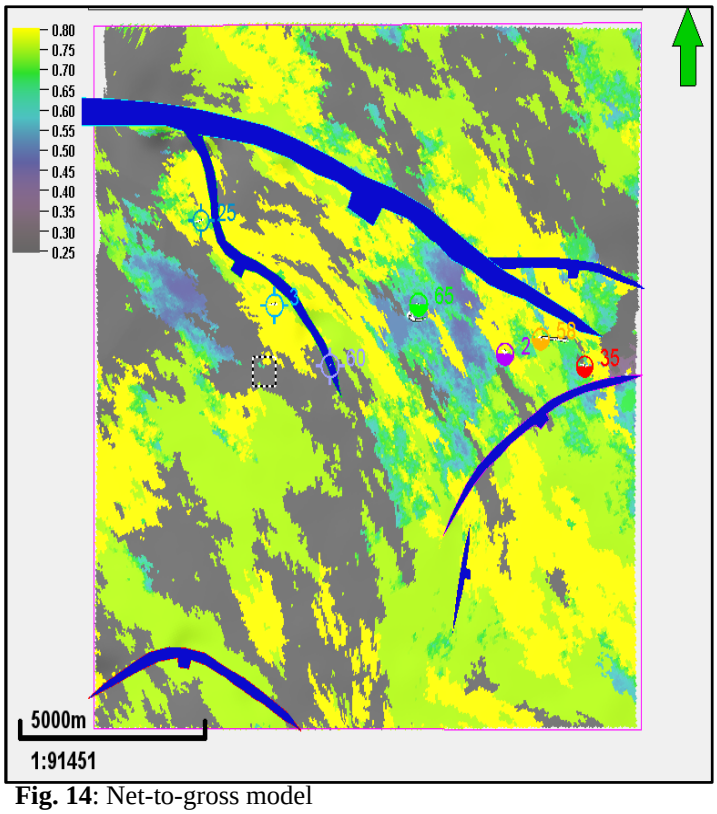


**Fig. 14**: Net-to-gross model

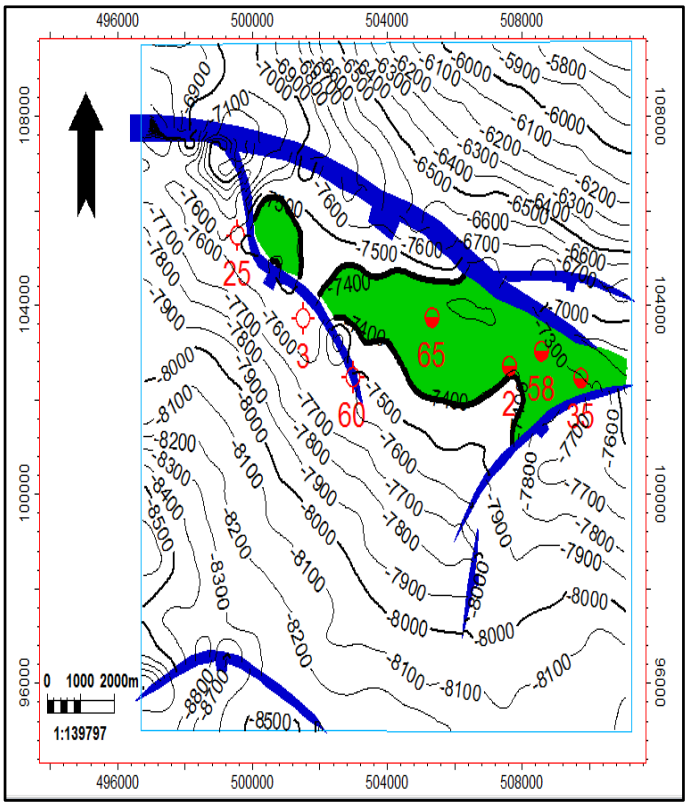


**Fig. 15:** Oil-water contact map

**Table 3:** Volumetric Estimation

| Reservoir | Bulk volume [acre. Ft] | Net volume [acre. Ft] | Pore volume [acre. Ft] | HCPV oil [acre. Ft] | STOIIP[STB] |
|---|---|---|---|---|---|
| **D_7** | 218,321 | 123,406 | 22,440 | 12,216 | 84,096,057 |
| **ZONES** | | | | | |
| **Zone 2** | 158,606 | 101,998 | 18,566 | 10,936 | 75,287,570 |
| **Zone 1** | 59,715 | 21,408 | 3,875 | 1,280 | 8,808,487 |

## V RECOMMENDATIONS

Conventional cores should be taken within the reservoir interval to further reduce uncertainties and validate the results obtained from the well logs. Detailed biostratigraphic analysis could be done to reliably interpret the depositional environment.

## VI. REFERENCES

Adaeze, I. U., Samuel, O.O., and Chukwuma, J.I., (2012). Petrophysical Evaluation of uzek well using well log and core data, Offshore Depobelt, Niger Delta, Nigeria. *Advances in Applied Science Research*, **3** (5):2966-2991

Archie, G.E. (1942). The electrical resistivity log as an aid in determining some reservoir characteristics. *Institute Petroleum Technology*.

Asquith, G. and Krygowski, D. (2004): Relationships of Well Log Interpretation in Basic Well Log Analysis Method in Exploration Series: *American Association of Petroleum Geologists*. l6**,** p l40.

Curtis, D.M., (1970). Miocene deltaic sedimentation, Louisiana Gulf Coast, in Deltaic sedimentation- Modern and ancient: *Soc. Econ. Paleontologist and Mineralogist Spec. Pub.* 15, pp. 293-308.

Damuth, J. E., (1994). Neogene gravity tectonics and depositional processes on the deep Niger Delta continental margin: *Marine and Petroleum Geology*, (11): 320– 346.

Doust, D.M. and Omatsola, E. (1990). Niger Delta. In Divergent/Passive Margin Basins, J.D. Edwards and P.A. Santogrossi, editors. *AAPG Memoir 48. American Association of Petroleum Geologists, Tulsa,* USA, pp. 239 – 248

Emmanuel, K. A., Clement, U. O., and Augustine, I. C., (2015). Integrated Workflow approach to static modeling of igloo R3 reservoir, onshore Niger Delta. *Interpretation*, **3**(3): SZ1 – SZ14. *https://doi.org/10.1190/INT-2014-0178.1*

Haldersen, H. H., and Dasleth, E., (1993). Challenges in Reservoir Characterization. *AAPG Bulletin*, **77**(1): 541-551.

Kulke, H., (1995). Nigeria, in H. Kulke, ed., Regional petroleum geology of the world. Part II: *Africa, America, Australia and Antarctica: Berlin, Gebruder Bornteaeger:* 143-172.

Lehner, P. and De Ruiter, P.A.C., (1977). Structural history of Atlantic Margin of Africa. *AAPG Bulletin.***61**: 961 – 981

Lucia, F. J., and Fogg, G. E., (1990). Geologic Stochastic Mapping of Heterogeneity in a Carbonate Reservoir. *Journal of Petroleum Technology*, **42**(1): 1298- 1303.

Mascle, J. R., B. D. Bornhold, and V. Renard, (1973). Diapiric structures off Niger delta: *American Association of Petroleum Geologists Bulletin.*, (57): 1672-1678.

Michelle L. W. T., Ronald R. C., and Michael E.B. (1999). The Niger Delta Petroleum System: Niger Delta Province, Nigeria, Cameroon, and Equatorial Guinea, Africa. *United State Geological Survey. Denver Colorado*: 4-70.

Oladipo, M. K., (2011). Integrated Reservoir Characterization: a case study of an onshore reservoir in Niger Delta basin. Pg. 24-25.

Oluwadare, O. A., Osunrinde, O. T., Abe, S. J., and Ojo, B. T., (2017). 3-D Geostatistical Model and Volumetric Estimation of 'Del' Field, Niger Delta. *Journal of Geology and Geophysics*, **6**(3). *DOI: 10.4172/2381-8719.1000291*

Oomkens, E., (1974). Lithofacies relations in the Late Quaternary Niger Delta Complex. *Sedimentology* (21): 195-222.

Reijers, T.J.A. (2011). Stratigraphy and Sedimentology of the Niger Delta. *Geologos, the Netherlands*, 17(3): 133-162.

Rider, M. H. (1986). The Geological Interpretation of Well Logs, Haistead Press, New York, NY, pp. 175 (SP, resistivity, induction, gamma, spectral gamma, gamma-gamma, neutron, acoustic).

Short, K. C., and Stauble, A. J., (1967). Outline of Geology of Niger Delta. *AAPG Bulletin*, **51**(1): 761-779.

Stacher, P., (1995). Present understanding of the Niger delta hydrocarbon habitat, In Oti, M. N. and Postma, G., (Eds). *Geology of deltas: Rotterdam, A.A. Balkema:* 257- 267.

Worthington, P. F., Lake, I. W., Carrol H. B., and Wesson, T. C., (1991). Reservoir characterization at the microscopic scale in reservoir characterization. *Academic Press, Waltham.* pp. 123-165.